Journal of Experimental Botany
https://doi.org/10.1093/jxb/erae310 Advance Access Publication 18 July 2024

RESEARCH PAPER

Source–sink relationships during grain filling in wheat in response to various temperature, water deficit, and nitrogen deficit regimes

Liang Fang[1], Paul C. Struik[1], Christine Girousse[2], Xinyou Yin[1,*], and Pierre Martre[3,*]

[1] Centre for Crop Systems Analysis, Wageningen University & Research, Wageningen, The Netherlands
[2] GDEC, INRAE, Clermont Auvergne University, Clermont-Ferrand, France
[3] LEPSE, Université Montpellier, INRAE, Institut Agro Montpellier, Montpellier, France

* Correspondence: xinyou.yin@wur.nl or pierre.martre@inrae.fr

Received 8 May 2024; Editorial decision 10 July 2024; Accepted 17 July 2024

Editor: Johannes Kromdijk, University of Cambridge, UK

Abstract

Grain filling is a critical process for improving crop production under adverse conditions caused by climate change. Here, using a quantitative method, we quantified post-anthesis source–sink relationships of a large dataset to assess the contribution of remobilized pre-anthesis assimilates to grain growth for both biomass and nitrogen. The dataset came from 13 years of semi-controlled field experimentation, in which six bread wheat genotypes were grown at plot scale under contrasting temperature, water, and nitrogen regimes. On average, grain biomass was ~10% higher than post-anthesis above-ground biomass accumulation across regimes and genotypes. Overall, the estimated relative contribution (%) of remobilized assimilates to grain biomass became increasingly significant with increasing stress intensity, ranging from virtually nil to 100%. This percentage was altered more by water and nitrogen regimes than by temperature, indicating the greater impact of water or nitrogen regimes relative to high temperatures under our experimental conditions. Relationships between grain nitrogen demand and post-anthesis nitrogen uptake were generally insensitive to environmental conditions, as there was always significant remobilization of nitrogen from vegetative organs, which helped to stabilize the amount of grain nitrogen. Moreover, variations in the relative contribution of remobilized assimilates with environmental variables were genotype dependent. Our analysis provides an overall picture of post-anthesis source–sink relationships and pre-anthesis assimilate contributions to grain filling across (non-)environmental factors, and highlights that designing wheat adaptation to climate change should account for complex multifactor interactions.

Keywords: Carbon, drought stress, extreme weather events, global warming, heat shock, nitrogen, remobilization, sink–source relationship, temperature, wheat.

Introduction

High temperatures and soil water deficit are the two most pervasive stresses for crop production. Besides average overall warming and increases in drought intensity associated with ongoing climate change, extreme heat waves and severe drought spells occur at a higher frequency. These climate change events are threatening global food production and lead to uncertainty

in global food supply in the future (Yin and Struik, 2017; Zhao *et al.*, 2017; Asseng *et al.*, 2019).

Yield of the grains harvested from cereal crops is co-determined by source (available net photosynthetic assimilates) and sink (the capacity of grains to utilize available assimilates) activities. There are dynamic feedback and feedforward interactions between source and sink; that is, the sink strength can influence source activity and *vice versa* (Martre *et al.*, 2003; Schapendonk *et al.*, 2007; Dingkuhn *et al.*, 2020; Reynolds *et al.*, 2022). Yet, source and sink respond differently to environmental variables (Yin *et al.*, 2009; Asseng *et al.*, 2017; Shi *et al.*, 2017; Shao *et al.*, 2021; Reynolds *et al.*, 2022). Therefore, quantifying how source and sink respond to different environmental variables and their interactions is essential when assessing the impacts of climate change and designing agricultural adaptation strategies.

Carbon assimilates for grain growth may come mainly from post-anthesis photosynthesis. High temperatures, including long-term elevated growth temperatures (HT) and short-term extremely high temperatures (heat shocks, HS) accelerate crop phenology and leaf senescence, thereby reducing the durations of photoassimilate accumulation and grain filling (Barnabás *et al.*, 2008; Asseng *et al.*, 2015, 2019). However, a higher grain-filling rate may partly compensate for the shorter grain-filling duration under moderately high temperatures (Yin *et al.*, 2009), but this may require an increased remobilization of (pre-anthesis) assimilate reserves stored in vegetative organs. Nevertheless, high temperatures that are within the supra-optimal range will suppress photosynthesis (Fang *et al.*, 2023). Water deficit (WD) suppresses photosynthesis mainly by reducing CO_2 diffusional conductance and limiting photosynthetic biochemical processes (Wei *et al.*, 2020; Fang *et al.*, 2023), but also via an accelerated whole-plant senescence (Evans, 1993). Yet, the effects of WD on grain-filling rate were inconsistent in previous studies where decreased (Yang *et al.*, 2006), unaffected (Nicolas *et al.*, 1984), and increased (Yang and Zhang, 2006) grain-filling rates under WD conditions were reported. Further, the impacts of high temperatures and water stress could be variable, depending on the timing of the stress occurrence (Stone and Nicolas, 1995; Winkel *et al.*, 1997). In addition to temperature and water supply, crop growth can be affected by other environmental factors (e.g. atmospheric CO_2 concentration and nitrogen supply; Rogers *et al.*, 1996; de Oliveira *et al.*, 2012; Shi *et al.*, 2017) and non-environmental factors (e.g. genotype; Eller *et al.*, 2020; Jiang *et al.*, 2022; Wang *et al.*, 2022).

Grain growth requires not only carbon but also nitrogen (Sinclair and de Wit, 1975). Thus, the concepts of source and sink cannot be applied merely to carbon assimilates, but should also include nitrogen (Martre *et al.*, 2003; Triboï *et al.*, 2003; Shao *et al.*, 2021). While grain nitrogen comes partially from post-anthesis nitrogen uptake, the remobilization of the pre-anthesis stored nitrogen in vegetative organs is known as the main source, and accounts for 50−100% of the final grain nitrogen (Papakosta and Gagianas, 1991; Gebbing and Schnyder, 1999; Kichey *et al.*, 2007; Shao *et al.*, 2021), depending on species, genotype, and growth conditions. Nonetheless, relatively little information is available on the responses of nitrogen source–sink relationships to environmental variables. Previous studies reported that environmental factors could influence nitrogen accumulation and remobilization (Palta *et al.*, 1994; Barbottin *et al.*, 2005). However, other studies suggested that environmental changes, such as global dimming (Shao *et al.*, 2021) and elevated temperature and elevated CO_2 (Wang *et al.*, 2019, 2020; Guo *et al.*, 2022), would not significantly influence nitrogen source–sink relationships or alter amounts of grain nitrogen (protein) in cereals such as wheat. Further systematic analyses are needed to reveal how environmental variables influence nitrogen budget in crops.

Wheat is one of the most important staple crops, annually producing >770 Mt of grains (FAOSTAT, 2022) and providing ~20% of the calories and protein in the human diet globally (Tilman *et al.*, 2011; Shiferaw *et al.*, 2013). Optimizing source–sink relationships is critical to improve wheat grain/nitrogen yield by ensuring a larger proportion of photoassimilates/nitrogen to the sink, particularly under adverse conditions. Numerous studies have documented the effects of various factors on the grain-filling process in wheat. Yet, probably due to the lack of accurate methodologies, few studies simultaneously compared source and sink during grain filling at crop scale. A method developed by Yin *et al.* (2009) and Shi *et al.* (2017) can quantify the source–sink relationships for both biomass and nitrogen during the post-anthesis phase, a key period determining final grain yield for cereals (Yang *et al.*, 2008). This method relies on data for the post-anthesis time course of dry mass for both total aboveground and grain mass, and its advantages have been discussed (Yin *et al.*, 2021). The method has been applied to several major annual crops (Shi *et al.*, 2017; Wei *et al.*, 2018; Shao *et al.*, 2021; Zhang *et al.*, 2022), for identifying genotypic or environmental factors that affect post-anthesis source–sink relationships.

Here, we used this method to analyze a large dataset of biomass and nitrogen dynamics during the post-anthesis period in six wheat genotypes grown under a total of 62 contrasting temperature, water, and nitrogen regimes across 13 independent experiments conducted in semi-controlled conditions under natural sunlight at INRAE, France. By making use of this large dataset, we aim at quantifying changes in wheat post-anthesis source and sink parameters under varying environmental regimes and providing an overview of wheat post-anthesis source–sink relationships under various environmental regimes. Such analyses would allow quantification of how contributions of remobilized pre-anthesis versus produced post-anthesis assimilates to grain growth can be affected by heat, WD, and low nitrogen supply (LN), and how genotypes differ in their strategies for coping with adverse environments.

Materials and methods

Semi-controlled field experiments

We analyzed a dataset from 13 experiments conducted in the (harvest) years of 1991, 1993, 1994, 1995, 1996, 1997, 1998, 1999, 2000, 2001, 2002, 2007, and 2014 (coded hereafter as EXP followed by year). Five winter wheat genotypes, Thésée (in EXP1991, EXP1993, EXP1994, EXP1995, EXP1996, EXP1997, and EXP1998), Renan (in EXP1999 and EXP2002), Récital (EXP2000, EXP2001, EXP2002, and EXP2007), Arche (in EXP2002), and Tamaro (in EXP2002), and a spring wheat line, SxB049 (in EXP2014) were grown. The latter was derived from a cross between the CIMMYT elite spring wheat genotypes Seri and Babax, and has been shown to better tolerate HT and WD, compared with its parents and sister lines (Pinto *et al.*, 2010) (see Fig. 1 for all treatment abbreviations). All experiments were conducted at Clermont-Ferrand, France (45°47'N, 3°10'E, 329 m elevation) in the Crop Climate Control and Gas Exchange Measurement (C3-GEM) platform.

In all experiments, plants were grown in 2 m^2 steel containers with 0.5 m depth, filled with a 2:1 (v: v) mixture of black soil and peat. Seeds were sown in November in most experiments (except in EXP1995 and EXP2014; see Supplementary Table S1 for detailed sowing dates for each experiment) at 2.5 cm from the soil surface with a density of 578 seeds m^{-2}, resulting in 329–634 plants m^{-2} at anthesis (within each experiment, plant densities were similar among treatments). The high plant density inhibited the development of axillary tillers which helped synchronize the development of the crops within and between the containers. The anthesis dates for most experiments were in May, regardless of genotype (Supplementary Table S1). Except for those cases where LN regimes were applied (see later), to avoid any nutrient deficiency, plants were fertilized several times at different growth stages and received a total of 15–33 g N m^{-2} (Supplementary Table S1). Plants were irrigated (in addition to receiving precipitation), whenever needed to maintain the soil water content above 80% of field capacity, except those regimes with WD (see later). For temperature treatments (see later), between 1 day before anthesis and 9 days after anthesis (DAA; depending on experiment and treatment; Fig. 1), each individual steel container was transferred from outside ambient conditions to a soil–plant–atmosphere research chamber with a closed air circulation. Chambers were covered by transparent polyethylene films where air temperature could be precisely controlled and natural precipitation could be excluded, allowing different temperature and water regimes to be applied (Triboï *et al.*, 1996). The solar radiation inside chambers was ~70% of that outside. Additionally, for other soil WD regimes without temperature manipulations (see later), the steel containers were transferred under a mobile rain-out shelter.

Environmental regimes

The descriptions of the temperature, WD, and LN regimes for all experiments are summarized in Fig. 1 and are described in Supplementary Table S1. The treatment codes include the final harvest year, genotype names, growth temperature regimes, and specific regimes, including heat shocks (HS), WD, elevated air CO_2 concentration (eCO_2), and LN. Arrows (→) indicate there was a temperature change from the original temperature (on the right of the arrow) to a new temperature (on the left of the arrow). Overall, the treatments in these experiments were divided into three factor groups, namely Temperature, Water, and Genotype. Within the Temperature group, experiments were designed to investigate the effects of either long-term changes in temperature during the post-anthesis period ($T_{post\text{-}anthesis}$) or short-term extremely high temperatures (i.e. HS) on source–sink relationships during the post-anthesis period. A brief description of the experiment groups is given below.

Long-term change in $T_{post\text{-}anthesis}$

Treatments in this group were to explore the effects of either elevated (HT) or lowered (LT) $T_{post\text{-}anthesis}$ (Supplementary Figs S1, S2). Due to the complexity of the temperature regimes, they were divided into three subgroups: (i) high growth temperature, including both constant and fluctuating (i.e. the temperature inside the enclosure chamber followed the outside ambient temperature with a fixed difference); (ii) diurnal thermal variability (i.e. contrasting day/night temperature); and (iii) change in fluctuating growth temperature during the grain-filling period.

(i) High growth temperature: in EXP1991 and EXP2000, constant high growth temperature regimes (28/20 °C and 28/15 °C for day/night in EXP1991 and EXP2000, respectively) were applied after anthesis.

(ii) Diurnal thermal variability: in EXP1993 and EXP1996, three different day/night temperature regimes were applied after anthesis: 18/10 °C (control), 34/10 °C, and 28/20 °C. In EXP1993, there was another regime, in which the 28/20 °C temperature conditions were combined with elevated atmospheric CO_2 (eCO_2; 700 ppm, compared with 380 ppm for the other treatments). In EXP2014, four different day/night temperature regimes were applied to the spring wheat line SxB049: 21/15 °C applied from 3 DAA to maturity (control), 22/20 °C applied from 3 DAA to maturity, 29/23 °C applied between 3 and 12 DAA (i.e. endosperm cell division phase) and then 21/15 °C until maturity, and 33/27 °C applied between 3 and 12 DAA and then 21/15 °C until maturity. In EXP1995, a constant 28/20 °C day/night temperature regime was implemented between 9 and 14 DAA, and then the temperature was increased to 34/10 °C until maturity.

(iii) Change in fluctuating growth temperature: in EXP1994, five fluctuating temperature regimes relative to ambient air temperature were applied: (1) outside ambient temperature (Out°C; control); (2) Out°C plus 5 °C ('Out+5°C'); (3) 'Out+5°C' until 18 DAA and then Out°C plus 10 °C ('Out+10°C') until maturity ('Out+5°C→Out+10°C'); (4) 'Out+10°C' until 16 DAA and then 'Out+5°C' until maturity ('Out+10°C→Out+5°C'); and (5) Out°C minus 5 °C ('Out–5°C'). In EXP1997, two temperature regimes were applied in two chambers, respectively: 'Out+10°C' until 22 DAA with 2 days of HS at 40 °C for 4 h at 13 and 14 DAA, then day/night temperature was controlled at 34/20 °C until maturity; 'Out–5°C' until 37 DAA, then day/night temperature was controlled at 18/10 °C until maturity (for this regime, 34/10 °C was applied in one of the chambers after 37 DAA; see Supplementary Table S1). For the 'Out+10°C' regime in EXP1994 and in EXP1997, except during the 2 days of HS, temperature was controlled below 35 °C and 34 °C, respectively; and for the 'Out–5°C' regime in EXP1994 and EXP1997 the temperature was controlled above 5 °C.

Short-term extremely high temperature (HS)

In this group, three experiments (EXP2001, EXP2007, and EXP2000) explored the effects of HS during the post-anthesis period, and whether the effects depend on the timing of HS (Supplementary Figs S1, S2). In EXP2000, plants were grown at 'Out–5°C' until 21 DAA, after which the temperature regime was changed to a constant day/night temperature of 18/10 °C. In EXP2001 and EXP2007, after anthesis all plant stands were maintained at a constant day/night temperature of 18/10 °C and 21/14 °C, respectively. Then HS were applied during the early grain-filling (HS1), mid grain-filling (HS2), and/or late grain-filling period (HS3). In EXP2001, HS, imposing 38 °C for 4 h (between 10.00 h and 14.00 h solar time) during a day of 20 °C for the remaining hours, was applied for four consecutive days from 7 to 10 DAA ('18/10°C HS1'), or from 18 to 21 DAA ('18/10°C HS2'). In EXP2007, HS, 38–40 °C imposed for 4 h (between 12.00 h and 16.00 h solar time) during a day of 21 °C for the remaining hours, was applied for four consecutive days from 8 to 11 DAA ('21/14°C HS1'), from 23 to 26 DAA ('21/14°C

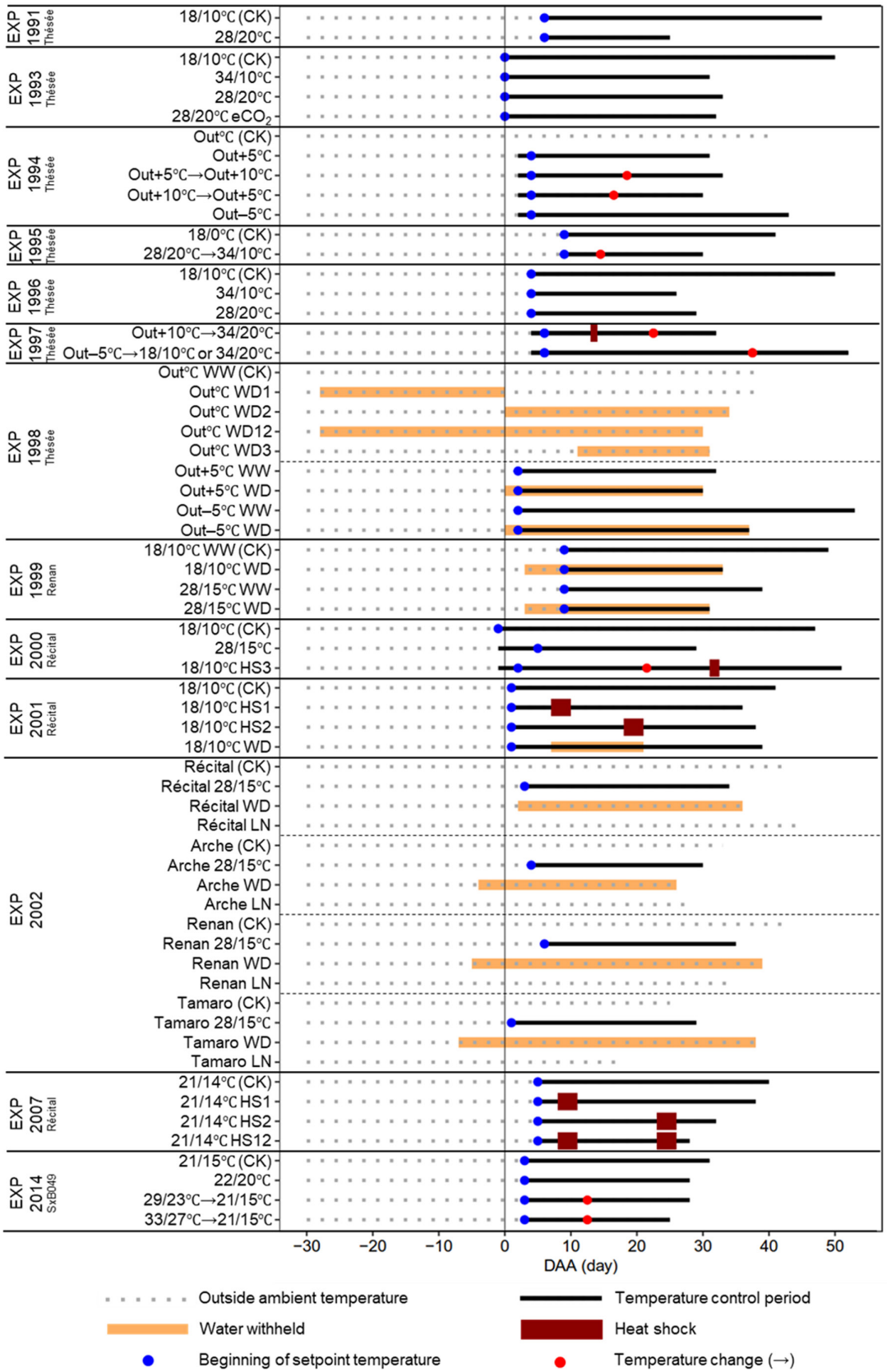

Fig. 1. Schema of the temperature, water deficit, and low nitrogen regimes tested in the 13 experiments analyzed in this study. In EXP1994, EXP1995, and EXP2000, before the beginning of setpoint temperature, plants were grown at 18/10 °C (day/night temperature) during the temperature control

period. In EXP2000, before temperature regimes changed to 18/10 °C, plants were grown at Out–5°C. Abbreviations and symbols: CK, control treatment; eCO_2, elevated air CO_2 concentration; Out°C, outside ambient temperature; Out+5°C, outside ambient temperature plus 5 °C; Out+10°C, outside ambient temperature plus 10 °C; Out–5°C, outside ambient temperature minus 5 °C; HS, heat shock; WW, well-watered; WD, water deficit; LN, low nitrogen. HS1, HS2, HS12, and HS3 represent heat shocks during the early grain-filling period, the mid grain-filling period, during both early and mid grain-filling periods, and during the late grain-filling period, respectively. WD1, WD2, WD12, and WD3 represent water deficit stress occurring during the pre-anthesis period, the post-anthesis period, both pre- and post-anthesis periods, and during the late grain-filling period, respectively. Details and codes for experiments and treatments on the left are defined in Supplementary Table S1.

HS2'), and for both periods ('21/14°C HS12'). In EXP2000, HS, 38 °C imposed on two consecutive days for 4 h (between 11.30 h and 14.30 h solar time) on the first day and for 6 h (between 10.15 h and 16.15 h) on the second day, was applied starting 30 DAA ('18/10°C HS3'). The rate of heating or cooling before and after the heat shocks was 4–9 °C h^{-1}.

Water

In this group, three experiments (EXP2001, EXP1999, and EXP1998) were included to explore the effects of WD on the source–sink relationship (Supplementary Figs S3, S4). We assessed whether or not the effects of WD would differ between pre- and post-anthesis periods, and also investigated the interactions between WD and HT. In EXP2001, water was withheld from 7 to 21 DAA, with day/night temperature controlled at 18/10 °C. EXP1999 aimed at analyzing WD by HT interactions. Day/night temperature was controlled at 18/10 °C and 28/20 °C starting 9 DAA under well-watered (WW) and WD conditions. The WD regimes were applied by withholding water from 3 DAA. In EXP1998, there were two sub-experiments. In the first sub-experiment, after anthesis two temperature settings relative to outside ambient temperature were applied in four containers ('Out+5°C' and 'Out–5°C'); for each temperature setting, one container was well irrigated and the other was subjected to WD treatment starting 0 DAA. In the second sub-experiment, plants of five containers were grown under outside ambient temperature; one container was well irrigated (control), and a WD treatment was applied in the other four containers during the pre-anthesis period (water withheld from 28 days before anthesis until anthesis, WD1), the post-anthesis period (water withheld from 0 DAA to maturity, WD2), both the post- and post-anthesis periods (WD12), and from mid grain filling to maturity (water withheld from 11 DAA to maturity, WD3). The total irrigation amount in each treatment in all the WD experiments is given in Supplementary Table S1.

Genotype

EXP2002 was conducted to investigate the genetic variability in the responses of source–sink relationship under different post-anthesis growth conditions. Four winter wheat genotypes (Récital, Arche, Renan, and Tamaro) with a contrasted ratio of leaf area index to grain number (Martre *et al.*, 2003), which is a proxy of the sink–source ratio (Supplementary Figs S5, S6), were grown under four different conditions: outside ambient temperature with WW (control), WD, and LN regimes, and a constant day/night temperature controlled at 28/20 °C (HT). In the WD regime, water was withheld from 7 d before anthesis and 2 DAA to maturity, depending on the anthesis date of each genotype, and in the LN regime no nitrogen was applied after the tillering stage.

Plant sampling and data collection

Plants were sampled every 2–9 days between anthesis and ripeness maturity. On each sampling date plants were collected on 0.2 × 1.0 m^2 starting from the north side of the plant stands. The plants were individualized and counted, and one to three replicates of 20 plants each were analyzed separately. Stems, leaf laminae, chaffs, and grains of each subsample were separated, and their dry mass was determined after drying to constant mass in a forced air oven at 80 °C. Total nitrogen concentration of oven-dried samples was determined by the Kjeldahl digestion method using a Kjeltec 2300 analyzer (Foss Tecator AB, Hoeganaes, Sweden) between 1991 and 2002, and by the Dumas combustion method using a FlashEA 19 1112 N/Protein analyzer (Thermo Electron Corp., Waltham, MA, USA) in 2007 and 2014.

Quantifying post-anthesis source–sink relationships

We quantified post-anthesis source–sink relationships in terms of either carbon or nitrogen, using the method developed by Yin *et al.* (2009) and Shi *et al.* (2017). Following their guideline, we used dry biomass data to analyze carbon source–sink relationships, as carbon fraction in biomass does not change significantly among plant organs in crops such as wheat, or among growth conditions (Penning de Vries *et al.*, 1989). In this method, sink parameters are estimated from the time course of grain dry mass or nitrogen during the grain-filling period, whereas source parameters are estimated from the dynamics of the total above-ground biomass or nitrogen mass (including senesced materials) during the same period. Thus, the 'source' in the method refers to biomass accumulated, or nitrogen taken up, only during the post-anthesis period; however, as described later, by comparing the post-anthesis 'source' supply with the post-anthesis grain 'sink' demand, the method does give an estimate of the contribution to grain growth of remobilized pre-anthesis assimilates (which usually are also considered as a 'source' to grain growth). In the method, the dynamics of both post-anthesis source and sink are described by a set of equations. To distinguish parameters, we use the subscripts 'si' and 'so' to indicate sink and source, respectively, throughout the text and equations. Symbols of all model parameters are defined in Table 1. Moreover, wherever appropriate, we use the subscripts 'M' and 'N' to indicate dry mass and nitrogen, respectively.

(i) Estimation of sink-related parameters: the dynamic data of either grain dry mass (g m^{-2}) or grain nitrogen (g m^{-2}) per unit ground area collected during the post-anthesis period can be described by a determinate sigmoid growth function (Yin *et al.*, 2003):

$$W_{si} = \begin{cases} (W_{x.si} - W_{b.si})\left(1 + \frac{t_{e.si} - t}{t_{e.si} - t_{m.si}}\right)\left(\frac{t - t_b}{t_{e.i} - t_b}\right)^{\frac{t_{e.si} - t_b}{t_{e.si} - t_{m.si}}} + W_{b.si} & \text{if } t_b \le t < t_{e.si} \\ W_{x.si} & \text{if } t \ge t_{e.si} \end{cases} \quad (1)$$

where t represents DAA, W_{si} is observed grain dry mass or nitrogen mass per unit ground area at time t, $W_{b.si}$ is the initial grain dry mass or nitrogen mass per unit ground area at anthesis (t_b), $W_{x.si}$ is the maximum grain dry mass or nitrogen mass per unit ground area when grain filling ends ($t_{e.si}$), and $t_{m.si}$ is the time when the maximum grain-filling rate is achieved (Fig. 2A). Here, we set t_b=0, as in earlier studies (Yin *et al.*, 2009; Shi *et al.*, 2017; Wei *et al.*, 2018; Shao *et al.*, 2021), and we also set $W_{b.si}$=0 as grain dry mass or nitrogen mass is expected to be close to zero at anthesis (i.e. the dry mass and nitrogen of ovules was neglected). After the parameters of Equation (1) were estimated by fitting the curves to the measured data, daily sink strength (Fig. 2B)—the rate of change in grain

Table 1. List of symbols of parameters of the source–sink model, and their definitions and units

Symbol	Definition	Unit
t	Days after anthesis	d
t_b	Anthesis date (denoted as days after anthesis, so, set as zero in the model)	d
$t_{m.si}$	Days after anthesis when the daily sink strength is maximal	d
$t_{e.si}$	Days after anthesis when the daily sink strength has decreased to zero. $t_{e.si.M}$ and $t_{e.si.N}$ represent $t_{e.si}$ for biomass and nitrogen, respectively	d
W_{si}	Observed grain dry mass or nitrogen mass per unit ground area	g m^{-2}
$W_{b.si}$	Initial grain dry mass or nitrogen mass at anthesis (set as zero in the model)	g m^{-2}
$W_{x.si}$	Maximum grain dry mass or nitrogen mass per unit of ground area	g m^{-2}
$s_{max.si}$	Maximum sink strength (i.e. maximum rate of grain filling)	g m^{-2} d^{-1}
$\bar{s}_{si}$	Mean sink strength (i.e. mean grain-filling rate) of the whole grain-filling period. $\bar{s}_{si.M}$ and $\bar{s}_{si.N}$ represent $\bar{s}_{si}$ for biomass and nitrogen, respectively	g m^{-2} d^{-1}
$S_{tot.si}$	Total sink demand of the whole grain-filling period. $S_{tot.si.M}$ and $S_{tot.si.N}$ represent $S_{tot.si}$ for biomass and nitrogen, respectively	g m^{-2}
$t_{m.so}$	Days after anthesis when the daily source activity declines at a maximum rate	d
$t_{e.so}$	Days after anthesis when the daily source activity has decreased to zero. $t_{e.so.M}$ and $t_{e.so.N}$ represent $t_{e.so}$ for biomass and nitrogen, respectively	d
W_{so}	Observed above-ground biomass or nitrogen mass per unit ground area	g m^{-2}
$W_{b.so}$	Above-ground biomass or nitrogen mass per unit ground area at anthesis	g m^{-2}
$W_{x.so}$	Maximum above-ground biomass or nitrogen mass per unit ground area at the end of grain filling	g m^{-2}
$s_{max.so}$	Maximum daily source activity, which is set to be achieved at the onset of grain filling	g m^{-2} d^{-1}
$\bar{s}_{so}$	Mean source activity of the whole grain-filling period. $\bar{s}_{so.M}$ and $\bar{s}_{so.N}$ represent $\bar{s}_{so}$ for biomass and nitrogen, respectively	g m^{-2} d^{-1}
$S_{tot.so}$	Total source supply of the whole grain-filling period. $S_{tot.so.M}$ and $S_{tot.so.N}$ represent $S_{tot.so}$ for biomass and nitrogen, respectively	g m^{-2}
RE	Contribution of remobilized pre-anthesis biomass (or nitrogen) needed to final grain dry biomass (or final grain nitrogen mass)	%

dry mass or nitrogen mass per unit area—can be calculated by the differential form of Equation (1), as:

$$\text{Sink strength} = \begin{cases} s_{max.si}\left(\frac{t_{e.si}-t}{t_{e.si}-t_{m.si}}\right)\left(\frac{t-t_b}{t_{m.si}-t_b}\right)^{\frac{t_{m.si}-t_b}{t_{e.si}-t_{m.si}}} & \text{if } t < t_{e.si} \\ 0 & \text{if } t \geq t_{e.si} \end{cases} \quad (2)$$

where $s_{max.si}$ is the maximum sink strength (g m^{-2} day^{-1}; i.e. the maximum grain-filling rate) at the time $t_{m.si}$ (DAA), which can be calculated as (Yin *et al.*, 2009):

$$s_{max.si} = (W_{x.si} - W_{b.si})\left[\frac{2t_{e.si} - t_{m.si} - t_b}{(t_{e.si} - t_{b.si})(t_{e.si} - t_{m.si})}\right]\left(\frac{t_{m.si} - t_b}{t_{e.si} - t_b}\right)^{\frac{t_{m.si}-t_b}{t_{e.si}-t_{m.si}}} \quad (3)$$

Further, the mean sink strength ($\bar{s}_{si}$, g m^{-2} day^{-1}, i.e. the mean grain-filling rate) during the whole grain-filling period can be calculated as:

$$\bar{s}_{si} = \frac{W_{x.si} - W_{b.si}}{t_{e.si} - t_b} \quad (4)$$

and the total sink demand ($S_{tot.si}$, g m^{-2}) during the whole grain-filling period can be calculated as (Yin *et al.*, 2021):

$$S_{tot.si} = W_{x.si} - W_{b.si} \quad (5)$$

Parameters described above could be applied to both dry mass and nitrogen data.

(ii) Estimation of source-related parameters: the source activity (g m^{-2} day^{-1}, i.e. the rate of change of above-ground biomass or nitrogen mass per unit ground area) declines during the grain-filling period (Fig. 2C), and this can be described by a reversed sigmoid model (Yin *et al.*, 2009):

$$\text{Source activity} = \begin{cases} s_{max.so}\left[1 - (1 + \frac{t_{e.so}-t}{t_{e.so}-t_{m.so}})\left(\frac{t}{t_{e.so}}\right)^{\frac{t_{e.so}}{t_{e.so}-t_{m.so}}}\right] & \text{if } t < t_{e.so} \\ 0 & \text{if } t \geq t_{e.so} \end{cases} \quad (6)$$

where $t_{e.so}$ is DAA when the source activity has decreased to zero, $t_{m.so}$ is DAA when the rate of decrease of source activity is maximum, and $s_{max.so}$ is the maximum source activity at the onset of the grain filling (g m^{-2} day^{-1}, i.e. the maximum rate of change of above-ground biomass or nitrogen mass per unit ground area). Integrating Equation (6) over time gives the following expression for the time course of above-ground biomass or nitrogen mass per unit ground area (g m^{-2}), W_{so}:

$$W_{so} = \begin{cases} s_{max.so}t\left[1 - \left(1 - \frac{t}{3t_{e.so} - 2t_{m.so}}\right)\left(\frac{t}{t_{e.o}}\right)^{\frac{t_{e.so}}{t_{e.so}-t_{m.so}}}\right] + W_{b.so} & \text{if } t < t_{e.so} \\ W_{x.o} & \text{if } t \geq t_{e.so} \end{cases} \quad (7)$$

Fitting Equation (7) to the data for the time course of above-ground biomass or nitrogen mass per unit ground area (Fig. 2D) gives an estimate of $s_{max.so}$ in addition to $t_{e.so}$ and $t_{m.so}$. By setting t=$t_{e.so}$, one can obtain from Equation (7) that $W_{x.so} - W_{b.so} = s_{max.so}\frac{t_{e.so}^2}{3t_{e.so} - 2t_{m.so}}$ (Yin *et al.*, 2009). Combining this with Equation (7) gives an alternative equation for W_{so}:

$$W_{so} = \begin{cases} \left[(W_{x.so} - W_{b.so})\frac{(3t_{e.so} - 2t_{m.so})t}{t_{e.so}^2}\right]\left[1 - \left(1 - \frac{t}{3t_{e.so} - 2t_{m.so}}\right)\left(\frac{t}{t_{e.so}}\right)^{\frac{t_{e.so}}{t_{e.so}-t_{m.so}}}\right] + W_{b.so} & \text{if } t < t_{e.so} \\ W_{x.so} & \text{if } t \geq t_{e.so} \end{cases} \quad (8)$$

where $W_{b.so}$ is the above-ground biomass or nitrogen per unit ground area at anthesis (g m^{-2}), and $W_{x.so}$ is the maximum above-ground biomass or nitrogen mass per unit ground area at the end of the growing season (g m^{-2}).

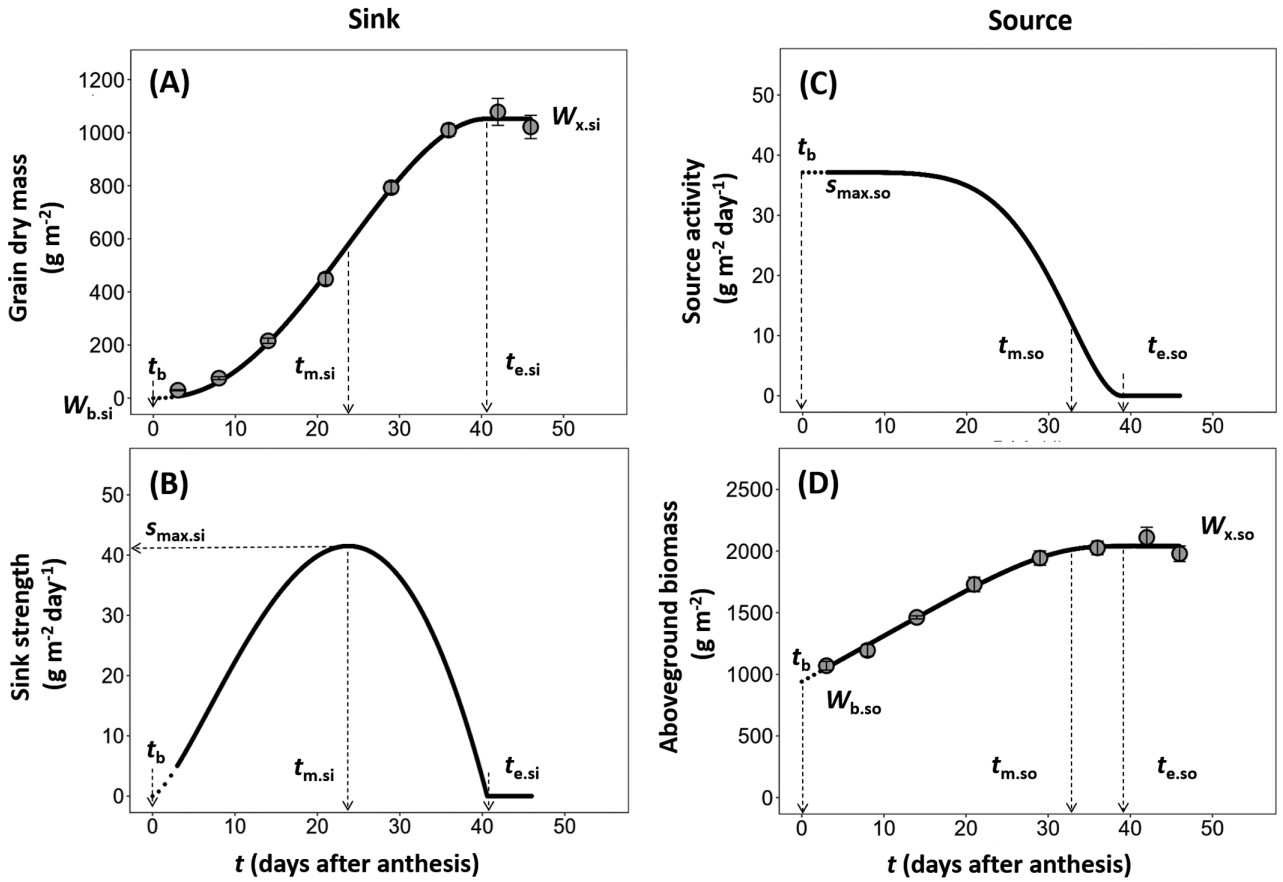

Fig. 2. Example of the post-anthesis time course of the measured grain dry mass and total above-ground biomass per unit area and the resulting dynamics of daily sink strength and source activity during grain filling. (A) Time course of grain dry mass during the post-anthesis period as described by Equation (1). (B) Dynamics of resulting daily sink strength during the post-anthesis period as described by Equation (2). (C) Dynamics of daily source activity during the post-anthesis period as described by Equation (6). (D) Time course of above-ground biomass during the post-anthesis period as described by Equation (8). The symbols of the model parameters are defined in Table 1. All time parameters are expressed as days after anthesis. Data used for this example illustration are for the winter wheat genotype Thésée grown under outside ambient temperature conditions (Out°C) in EXP1994. In (A) and (D), circles and errors bars are means ±SE of three replicates.

The mean source activity ($\bar{s}_{so}$, g m^{-2} day^{-1}) during the whole grain-filling period can be calculated as:

$$\bar{s}_{so} = \frac{W_{x.so} - W_{b.so}}{t_{e.so} - t_b} \quad (9)$$

and the total source supply ($S_{tot.so}$, g m^{-2}) during the whole grain-filling period can be calculated as:

$$S_{tot.so} = W_{x.so} - W_{b.so} \quad (10)$$

(iii) Statistical analysis of source–sink balance: the post-anthesis source/sink ratio was defined as $S_{tot.so}/S_{tot.si}$ and the post-anthesis source–sink difference was calculated as ($S_{tot.so}$–$S_{tot.si}$). The common procedure for estimating source and sink parameters was to fit Equation (8) and Equation (1) separately, which would fail to statistically test whether or not $S_{tot.so}$ (i.e. $W_{x.so}$–$W_{b.so}$) and $S_{tot.si}$ (i.e. $W_{x.si}$–$W_{b.si}$) are balanced. To solve this problem, following Shao *et al.* (2021), we introduced dummy variables (Z_1 and Z_2) and defined them using binary values in such a way that Z_1=1 and Z_2=0 corresponds to the source whereas Z_1=0 and Z_2=1 represents the sink:

$$W = Z_1 W_{so} + Z_2 W_{si} \quad (11)$$

By combining Equations (1) and (8) with Equation (11), all parameters in Equations (1) and (8) can be estimated simultaneously in a single procedure by fitting observed data of the time course of both W_{so} and W_{si} (the full model) (see an example in Supplementary Protocol S1 on how dummy variable values were given). Then, we set a null hypothesis (H_0) that $S_{tot.so}$ mathematically equals $S_{tot.si}$ (i.e. post-anthesis source and sink are balanced), which gives:

$$W_{x.so} = W_{x.si} - W_{b.si} + W_{b.so} \quad (12)$$

We incorporated Equation (12) into the fitting procedure, thereby removing $W_{x.so}$ from parameters to be fitted (reduced model). By comparing the residual sum of squares and degrees of freedom between the two sets of fitting for the full model and the reduced model, we performed an *F*-test to test whether or not the total post-anthesis

source and sink are significantly different. An insignificant *F*-value at P=0.05 meant to accept the H_0; that is, post-anthesis source and sink are balanced.

(iv) Quantifying remobilization: while the method, as stated earlier, does not explicitly include pre-anthesis assimilates as a 'source' term, it does allow us to quantify the required remobilization of pre-anthesis assimilates/nitrogen to support grain (sink) growth. The contribution of pre-anthesis (RE, %) carbon assimilates or nitrogen to the sink is given by:

$$\mathrm{RE} = \frac{S_{\mathrm{tot.si}} - S_{\mathrm{tot.so}}}{S_{\mathrm{tot.si}}} \times 100 \tag{13}$$

It should be noted that Equation (13) works best when $S_{\mathrm{tot.si}} \geq S_{\mathrm{tot.so}}$. When $S_{\mathrm{tot.si}} > S_{\mathrm{tot.so}}$ then post-anthesis production does not suffice and a remobilization of pre-anthesis reserves is required and the required RE (%) is as calculated by Equation (13). When $S_{\mathrm{tot.si}} = S_{\mathrm{tot.so}}$, then post-anthesis production just suffices for the grain demand and the required RE is 0%. When $S_{\mathrm{tot.si}} < S_{\mathrm{tot.so}}$, however, the term ($S_{\mathrm{tot.si}} - S_{\mathrm{tot.so}}$) and RE are negative, meaning that the post-anthesis source supply has a surplus relative to sink demand and there is no remobilization of pre-anthesis assimilates needed. The absolute value of this difference can be interpreted as the surplus that will add to the existing pre-anthesis reserves.

The framework as described was to analyze data for post-anthesis above-ground as well as grain dynamics in order to quantify the post-anthesis source–sink relationships and pre-anthesis reserve contribution (RE, %) to grain growth. It assumes that grains are the predominant above-ground sink during grain filling. Strictly speaking, when stems and leaves are also sinks to some extent, the calculated RE, if zero or even negative, does not mean that remobilization did not occur at all. Similarly, if RE is above zero, it does not mean that the actual total remobilization is that number. However, our calculated RE (%) conclusively quantifies the 'net' remobilization that is needed to contribute to grain growth. Also, the method could ideally be applied to estimate the source parameters using the whole-plant biomass or N data (that includes roots). However, measuring below-ground dynamics is practically infeasible at a large scale. Environmental variables may alter root dynamics during the post-anthesis phase. If this indeed occurred, our estimated $S_{\mathrm{tot.so}}$ would represent either the gross (post-anthesis production plus remobilization from roots if roots 'export') or the net (post-anthesis production minus partitioning to roots if roots 'import') post-anthesis assimilate supply for above-ground growth. In either case, the term ($S_{\mathrm{tot.si}} - S_{\mathrm{tot.so}}$) does not change if grains are indeed the predominant sink for available above-ground assimilates during grain filling. As a result, RE (referring to the contribution of pre-anthesis above-ground reserves to grains) would become somewhat smaller if roots 'export' and somewhat larger if roots 'import'.

Curve fitting

Non-linear curve fitting procedures were implemented using the GAUSS method in PROC NLIN of the statistical software SAS version 9.4 (SAS Institute Inc, Cary, NC, USA). The SAS codes can be found in Supplementary Protocol S1. We performed the fitting, using pooled data of individual replicates to obtain estimates of parameters which are most reliable for representing treatment-specific parameters (which in fact are close to the mean of replicated estimates but have better statistical predictions of all data points than the mean). In the cases where overfitting occurred, we fixed the value of $t_{\mathrm{e.so}}$ at the first data point where a plateau (the maximum value) was observed. $W_{\mathrm{b.so}}$ represents the initial above-ground biomass or nitrogen mass at anthesis, and its value is assumed to be identical among treatments that were applied after anthesis. Thus, to minimize errors, in each year, for those treatments applied after anthesis, curve fitting was first performed within each treatment, and then data were re-fitted by fixing $W_{\mathrm{b.so}}$ at the mean value of $W_{\mathrm{b.so}}$ across treatments.

In EXP1997, although day/night temperatures were changed to 18/10 °C and 34/10 °C after 'Out–5°C' at 37 DAA in two chambers, respectively, the data showed little difference; therefore, data collected from the two plant stands with the same regime ('Out+10°C→34/20°C') or similar regimes ('Out–5°C→18/10°C' and 'Out–5°C→34/10°C') were pooled together to be fitted. In EXP2002, the above-ground biomass of Tamaro initially increased but later decreased after reaching a peak (~400 °Cd to 500 °Cd, depending on treatments), while at the same time the grain biomass was still increasing. The decreased above-ground biomass during the later grain-filling period resulted in very little above-ground biomass accumulation over the whole grain-filling period. Similarly, the amount of above-ground nitrogen was relatively constant during the post-anthesis period. Thus, we assumed that the total source supply for biomass or nitrogen during the post-anthesis period was zero for Tamaro.

Results

The model described well the dynamics of post-anthesis source and sink

By using the method developed by Yin *et al.* (2009) and Shi *et al.* (2017), we quantified post-anthesis source, sink, and their relationships in 13 independent experiments (see Fig. 1 for experimental regimes). As stated earlier, source supply for grain filling is usually defined as the sum of the pre-anthesis stored carbohydrates and the post-anthesis produced assimilates (Asseng *et al.*, 2017; Reynolds *et al.*, 2022). Here, based on our modeling framework, we parameterized source only based on the biomass produced or nitrogen accumulated after anthesis. As illustrated in Fig. 2, the dynamics of post-anthesis sink and source were well described by the model [Equations (1) and (8)], with an average R^2 of 0.943 ± 0.017 (n=62) for biomass and of 0.922 ± 0.020 (n=39) for nitrogen.

Relations for biomass

Both $S_{\mathrm{tot.si.M}}$ and $S_{\mathrm{tot.so.M}}$ varied with experiments and environmental regimes (Fig. 3A). On average $S_{\mathrm{tot.si.M}}$ was ~10% higher than $S_{\mathrm{tot.so.M}}$, indicating that overall, the remobilization of pre-anthesis reserves was required. However, the calculated average RE for biomass varied from –19% to 100% (depending on experiments and environmental regimes) with a mean value of 22% (Supplementary Figs S1B, S3B, S5B). The plot of Fig. 4A appeared to identify a value of $S_{\mathrm{tot.si.M}}$ (~950 g m^{-2}). Below this value, pre-anthesis stored carbon assimilates increasingly contributed to the grain biomass. Above the value, post-anthesis photoassimilates were in a slight excess of the demand for grain filling, as shown by negative values of RE calculated by Equation (13).

Both short-term HS (4 h at 38 °C for 2–4 days) and long-term temperature elevation (HT) reduced $S_{\mathrm{tot.so.M}}$ and $S_{\mathrm{tot.si.M}}$, but in general HT had larger effects than HS (Supplementary Fig. S1A). The impacts of HT on $S_{\mathrm{tot.so.M}}$ and $S_{\mathrm{tot.si.M}}$ varied among regimes. For instance, $S_{\mathrm{tot.so.M}}$ and

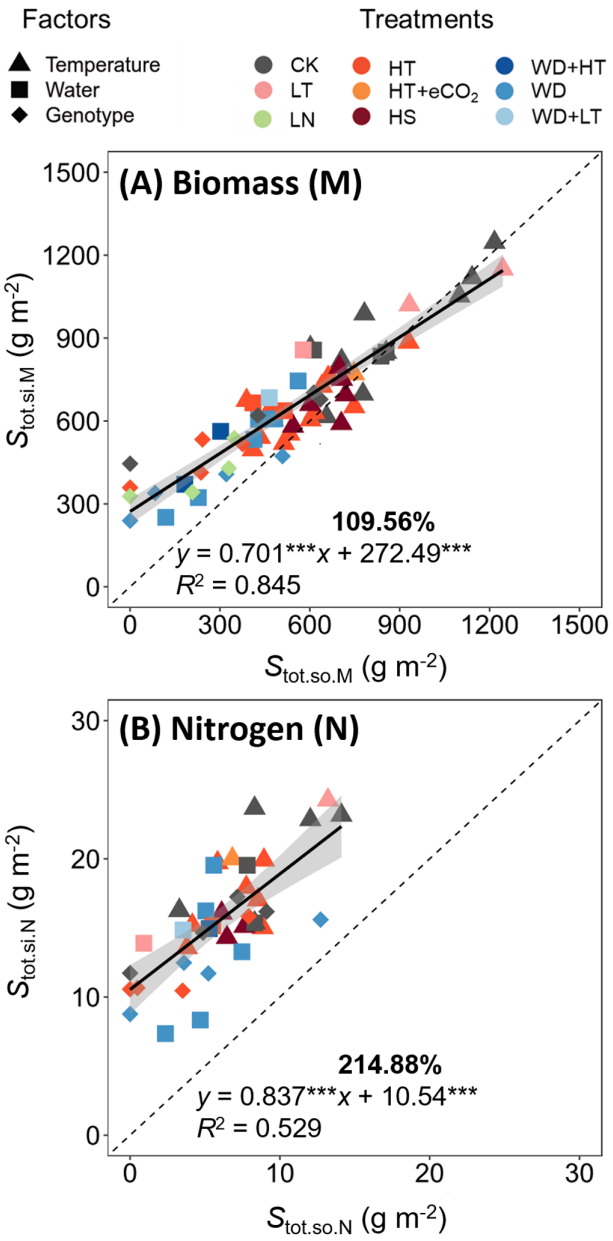

Fig. 3. Relationships between post-anthesis source and sink. Total post-anthesis source supply ($S_{tot.so}$) and total sink demand ($S_{tot.si}$) for biomass (A) and nitrogen (B) are plotted for winter wheat cultivars grown under different temperature, water deficit, and low nitrogen regimes. The shaded area depicts the 95% confidence interval of the predictions. Dashed lines are the 1:1 relationship. The full lines represent regression equations (significant at $P<0.001$). The bold number (%) above the regression equation in each panel is the average of *y*-axis relative to *x*-axis values across regimes. Data are for factors of 'Temperature' (long-term temperature changes and short-term heat shocks regimes; Supplementary Figs S1, S2), 'Water' (water supply regimes; Supplementary Figs S3, S4), and 'Genotype' (the wheat genotypes Thésée, Récital, Renan, Arche, and Tamaro grown under high temperature, water deficit, and low nitrogen regimes; Supplementary Figs S5, S6). CK, control treatment; LT, low growth temperature (Out–5°C); HT, high growth temperature; eCO_2, elevated air CO_2 concentration; HS, heat shock; WD, water deficit stress; LN, low nitrogen supply.

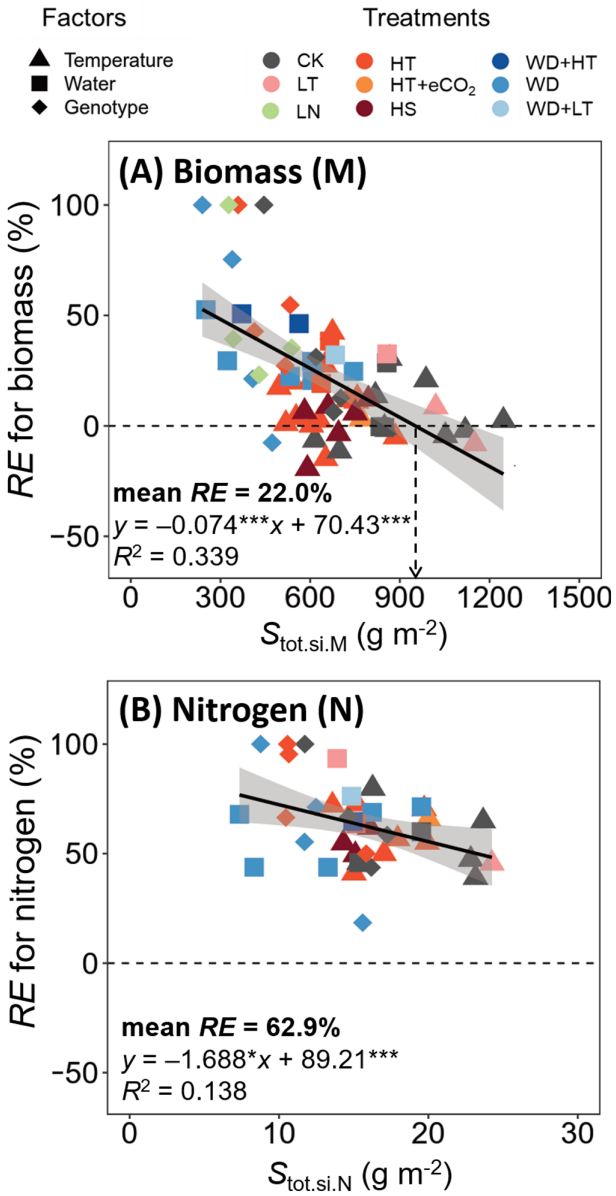

Fig. 4. The required contribution (%) of remobilized pre-anthesis assimilates to grain growth (RE) versus grain sink demand. This is shown for biomass (A, where the *x*-axis is total grain biomass $S_{tot.si,M}$) and for nitrogen (B, where the *x*-axis is total grain nitrogen $S_{tot.si,N}$), based on the pooled results for winter wheat cultivars grown under different temperature, water deficit, and low nitrogen regimes. The shaded area depicts the 95% confidence interval of the predictions. The full lines represent regression equations (* and *** significant at $P<0.05$ and 0.001, respectively). Dashed horizontal lines indicate the case when RE=0%, while the dashed vertical line in (A) identifies a value of $S_{tot.si,M}$ below which RE is >0% and above which RE is <0%. The bold value in each panel is the mean RE across regimes. Symbols for experimental factors are identified as in Fig. 3. The extreme values of RE at 100% in (A) are for cv. Tamaro, which hardly accumulated above-ground biomass during the whole grain-filling period such that its grain growth relied entirely on remobilized assimilates (see the text). As $S_{tot.si,M}$ and $S_{tot.si,N}$ decreased with increasing stress intensity, this figure suggests that the remobilization of pre-anthesis reserves became increasingly important for grain growth with increasing stress intensity, as discussed in the text.

$S_{tot.si.M}$ were more reduced by 34/10 °C than by 28/20 °C (EXP1993 and EXP1996 in Supplementary Fig. S1A), even though $T_{post\text{-}anthesis}$ was identical between the two temperature regimes. Elevated CO_2 slightly mitigated the negative impact of 28/20 °C on $S_{tot.so.M}$ but not that on $S_{tot.si.M}$ (EXP1993 in Supplementary Fig. S1A). Also, high night temperature (22/20 °C) did not affect $S_{tot.so.M}$ and $S_{tot.si.M}$ (EXP2014 in Supplementary Fig. S1A). Two to four days of HS did not change relative values of $S_{tot.so.M}$ and $S_{tot.si.M}$, regardless of the timing when HS were applied (Fig. 3A; Supplementary Fig. S1A). Likewise, HT had limited impacts on the differences between $S_{tot.so.M}$ and $S_{tot.si.M}$ (Fig. 3A). For example, in many cases (EXP1993, EXP1994, EXP1995, EXP1997, EXP2000, and EXP2014), the $S_{tot.so.M}$–$S_{tot.si.M}$ difference was not significant, and thus RE for biomass was low (Supplementary Fig. S1A, B).

WD and LN, particularly WD, had profound impacts on the relative differences between $S_{tot.so.M}$ and $S_{tot.si.M}$, with $S_{tot.so.M}$ being significantly lower than $S_{tot.si.M}$; therefore, high RE values for biomass were observed in these regimes (Fig. 4A; Supplementary Figs S3B, S5B). The impact of WD on $S_{tot.so.M}$ and $S_{tot.si.M}$ depended on the timing of WD. For example, in EXP1998, compared with WD2 (water withheld from 0 DAA to maturity), WD1 (water withheld from 28 days before anthesis to anthesis) had greater impacts on $S_{tot.so.M}$ and $S_{tot.si.M}$ (Supplementary Fig. S3A). Moreover, the impact of WD on biomass was larger under HT than under ambient temperature. In EXP1999, $S_{tot.so.M}$ and $S_{tot.si.M}$ were reduced by 42% and 27% under WD regimes compared with the WW regime, respectively; and the combination of HT (28/15 °C) and WD reduced $S_{tot.so.M}$ and $S_{tot.si.M}$ by 78% and 55%, respectively (Supplementary Fig. S3A). Similar results were also found in EXP1998 (Supplementary Fig. S3A).

Post-anthesis biomass source and sink parameters were also genotype dependent. Under ambient control conditions (CK), Arche, Récital, Renan, and Tamaro showed contrasting $S_{tot.so.M}/S_{tot.si.M}$ ratios, with Arche having the highest ratio and Tamaro having the lowest ratio (Supplementary Fig. S5A), which confirmed results observed in the field (Martre *et al.*, 2003). Although HT, WD, and LN all reduced $S_{tot.so.M}$ and $S_{tot.si.M}$, their impacts varied among genotypes. For instance, WD decreased $S_{tot.si.M}$ for Arche, Récital, and Renan by 30, 42, and 45%, respectively. However, under WD, $S_{tot.so.M}$ for Arche remained relatively high (it decreased by only 20% compared with CK), which was not the case for Récital and Renan ($S_{tot.so.M}$ decreased by 48% and 80% for Récital and Renan, respectively). These resulted in a decrease in the $S_{tot.so.M}/S_{tot.si.M}$ ratio for Récital and Renan and in an increased ratio for Arche (Supplementary Fig. S5A). Additionally, RE values for biomass were always observed for Récital, Renan, and Tamaro, regardless of growth conditions, while for Arche RE was substantial only under HT and LN (Supplementary Fig. S5B).

Relationships for nitrogen

Like $S_{tot.si.M}$ and $S_{tot.so.M}$, both $S_{tot.si.N}$ and $S_{tot.so.N}$ varied with the studied factors and environmental regimes (Fig. 3A). In all regimes, $S_{tot.si.N}$ was significantly higher than $S_{tot.so.N}$ (Supplementary Figs S2A, S4A, S6A), and overall $S_{tot.si.N}$ was as high as 215% of $S_{tot.so.N}$ (Fig. 3B). Thus, high RE values for nitrogen were observed in all cases, ranging from 18% to 100% with an average of 63% (Fig. 4B; Supplementary Figs S2B, S4B, S6B).

Environmental regimes (e.g. HT, HS, and WD) did not markedly affect the relationships between $S_{tot.so.N}$ and $S_{tot.si.N}$, but genotype and its interaction with environmental regimes did (Supplementary Fig. S6). For instance, HT decreased both $S_{tot.so.N}$ and $S_{tot.si.N}$ for Récital by 90% and 27%, respectively, and for Arche by 62% and 35%, respectively (Supplementary Fig. S6A); whereas for Renan, HT did not significantly decrease $S_{tot.so.N}$ and $S_{tot.si.N}$ (Supplementary Fig. S6A). WD markedly decreased $S_{tot.so.N}$ and $S_{tot.si.N}$ for Renan (by 27% and 32%, respectively), but had limited impacts on those for Arche where $S_{tot.so.N}$ even increased by 40% under WD (Supplementary Fig. S6A).

Temperature responses of estimated parameters

For biomass, under WW and non-limiting nitrogen (HN) regimes, both $S_{tot.so.M}$ and $t_{e.so.M}$ decreased with increasing $T_{post\text{-}anthesis}$ (Fig. 5A, B). In most WD and LN regimes, the values of both $S_{tot.so.M}$ and $t_{e.so.M}$ were lower than expected from their temperature response. $\bar{s}_{so,M}$ was not significantly correlated with $T_{post\text{-}anthesis}$, and averaged 18 g m^{-2} day^{-1} for WW and HN regimes and 12 g m^{-2} day^{-1} for WD and LN regimes (Fig. 5C). As for the sink parameters, $S_{tot.si.M}$ and $t_{e.si.M}$ were negatively correlated with $T_{post\text{-}anthesis}$ under WW and HN regimes (Fig. 5D, E). In most WD and LN regimes, $S_{tot.si.M}$ was lower than expected from its temperature response. $t_{e.si.M}$ was less reduced in WD and LN regimes than $S_{tot.si.M}$ (Fig. 5D, E). $\bar{s}_{si.M}$ was not significantly correlated with $T_{post\text{-}anthesis}$ (Fig. 5F), and averaged 20 g m^{-2} day^{-1} for WW and HN regimes and 14 g m^{-2} day^{-1} for WD and LN regimes. *F*-test analysis showed that under WW and HN regimes $S_{tot.so.M}$ and $S_{tot.si.M}$ (Fig. 5A, D) had a similar response to $T_{post\text{-}anthesis}$. The difference between $S_{tot.so.M}$ and $S_{tot.si.M}$ (Fig. 5G), the ratio of $S_{tot.so.M}$ to $S_{tot.si.M}$ (Fig. 5H), and RE for biomass (Fig. 5I) were not significantly correlated with $T_{post\text{-}anthesis}$, irrespective of water and nitrogen regimes. RE for biomass averaged 15% for WW and HN regimes and 41% for WD and LN regimes (Fig. 5I).

For nitrogen parameters, $S_{tot.so.N}$ and $S_{tot.si.N}$, and their difference and ratio, were not significantly correlated with $T_{post\text{-}anthesis}$, regardless of water regimes (Fig. 6A, D, G, H). Both $t_{e.so.N}$ (Fig. 6B) and $t_{e.si.N}$ (Fig. 6E) decreased as $T_{post\text{-}anthesis}$ increased under both WW and WD regimes, and WD slightly modified the temperature responses of $t_{e.so.N}$ and

$t_{e.si.N}$. $\bar{s}_{si.N}$, but not $\bar{s}_{so.N}$, showed significantly positive correlation ($P<0.01$) with $T_{post\text{-}anthesis}$ under WW and HN regimes (Fig. 6C, F).

Discussion

With a quantitative analysis of post-anthesis biomass and nitrogen accumulation for several wheat genotypes grown in a large set of experiments, we were able to systematically investigate to what extent post-anthesis source and sink parameters for biomass and nitrogen can be affected by temperature, water, and nitrogen regimes, and genotype.

High temperatures had little impact on post-anthesis biomass relationships

Pooling the results across all experiments gave an overall picture of post-anthesis biomass source supply versus sink demand across factors and environmental regimes (Fig. 3A). The relationship shown in Fig. 4A identified a grain yield value (equivalent to $S_{tot.si.M}$ being ~950 g m^{-2}) at and above which (mostly under CK and LT conditions) no remobilization of pre-anthesis stored assimilates was required. Under adverse conditions (mainly under WD and LN conditions) when grain yield was lower than ~950 g m^{-2}, post-anthesis source supply was insufficient in support of sink demand, leading to an increasing contribution of remobilized pre-anthesis assimilates to grain yield (Fig. 4A).

However, there was little effect of HS on total post-anthesis source supply ($S_{tot.so.M}$) and sink demand ($S_{tot.si.M}$) in most cases. Instead, it was the average post-anthesis temperature ($T_{post\text{-}anthesis}$) that played a predominant role. Our results suggested that $S_{tot.so.M}$ and $S_{tot.si.M}$ decreased similarly with increasing $T_{post\text{-}anthesis}$ under WW and HN regimes (Fig. 5A, D), and these decreases were determined more by the post-anthesis durations ($t_{e.so.M}$ and $t_{e.si.M}$; Fig. 5B, E) than by the mean rates of source supply ($\bar{s}_{so.M}$) and sink demand ($\bar{s}_{si.M}$) (Fig. 5C, F). These results were in line with the common observation that the acceleration of phenology is the primary driver of the negative impact of rising temperatures on crop production, because the shortened growing period will result in less time for carbon assimilation and grain filling, eventually leading to yield loss (Wardlaw and Moncur, 1995; Zhao *et al.*, 2007; Liu *et al.*, 2014; Asseng *et al.*, 2015, 2019). HS did not lead to obvious deviations in the temperature response curves of source and sink parameters. Moreover, the relatively constant source supply rate ($\bar{s}_{so.M}$) across $T_{post\text{-}anthesis}$ may be partially attributed to the low sensitivity of canopy photosynthetic rate to increasing air temperatures, due to the cooling effect by evapotranspiration, at canopy scale under WW conditions (Webber *et al.*, 2017). It could also result from the remobilization of carbohydrates from below-ground to above-ground under adverse conditions during grain filling (Palta *et al.*, 1994), or could be explained by other factors, such as the in-season variations of solar radiation (Asseng *et al.*, 2017; Shao *et al.*, 2021) and diurnal temperature variations (Asseng *et al.*, 2015). The relatively constant sink demand rate ($\bar{s}_{si.M}$) at different $T_{post\text{-}anthesis}$ is in contrast to previous experimental observations at single-plant level where wheat grain-filling rate was affected by temperature (Yin *et al.*, 2009). The relatively smaller variations of $\bar{s}_{si.M}$ (Fig. 5F) compared with $\bar{s}_{so.M}$ (Fig. 5C) could have been due to compensations by pre-anthesis assimilate remobilization.

The temperature responses of total post-anthesis source supply ($S_{tot.so.M}$) and sink demand ($S_{tot.si.M}$) were downward shifted under WD and LN regimes (Fig. 5A, D). Yet, the extent of the shift was stronger for $S_{tot.so.M}$ than for $S_{tot.si.M}$, as a result of higher remobilization (RE%) under WD and LN regimes. Like high temperatures, WD accelerates senescence (Evans, 1993; Farooq *et al.*, 2014) and decreases photosynthesis (Liu *et al.*, 2019; Wei *et al.*, 2020, 2022; Fang *et al.*, 2023). However, in contrast to some previous findings that WD hardly affects or slightly increases grain-filling rate (Nicolas *et al.*, 1984; Yang and Zhang, 2006), here the rates (both $\bar{s}_{so.M}$ and $\bar{s}_{si.M}$) were suppressed across $T_{post\text{-}anthesis}$ under WD or LN regimes, resulting in the lower biomass accumulation ($S_{tot.so.M}$ and $S_{tot.si.M}$) (Fig. 5A–F).

Under natural field conditions, heat and drought often concurrently occur (i.e. compound stresses), leading to difficulties in identifying the separate impacts of heat and drought (Lesk *et al.*, 2022). Consequently, the impact of heat stress may be overestimated. Here, our results revealed that WD and the combined WD and HT exerted a more profound impact on wheat biomass sink–source relationships than HT alone (Fig. 3A). This is in line with our previous finding at leaf scale that post-anthesis drought exerts a greater impact on photosynthesis than post-anthesis heat (Fang *et al.*, 2023).

Post-anthesis nitrogen relationships hardly responded to temperature and water regimes

Unlike the source of grain biomass that is mainly produced after anthesis, the source of grain nitrogen mainly comes from the nitrogen uptake before anthesis (Papakosta and Gagianas, 1991; Gebbing and Schnyder, 1999; Shao *et al.*, 2021), which was also supported by our study. On average, RE across all environmental regimes and genotypes was 22% for biomass (Fig. 4A) and 63% for nitrogen (Fig. 4B). In line with the higher RE for nitrogen, the mean rate of grain nitrogen accumulation ($\bar{s}_{si.N}$) was higher than the mean rate of post-anthesis nitrogen uptake ($\bar{s}_{so.N}$) (Supplementary Fig. S7D). Our results suggest that the discrepancy between the rates of grain nitrogen demand and post-anthesis nitrogen uptake was independent of the post-anthesis duration (Supplementary Fig. S7B).

Some earlier studies showed that wheat nitrogen fluxes were influenced by environmental changes (Palta *et al.*, 1994; Barbottin *et al.*, 2005). However, while our study could not identify the effect of LN due to the lack of data, we found

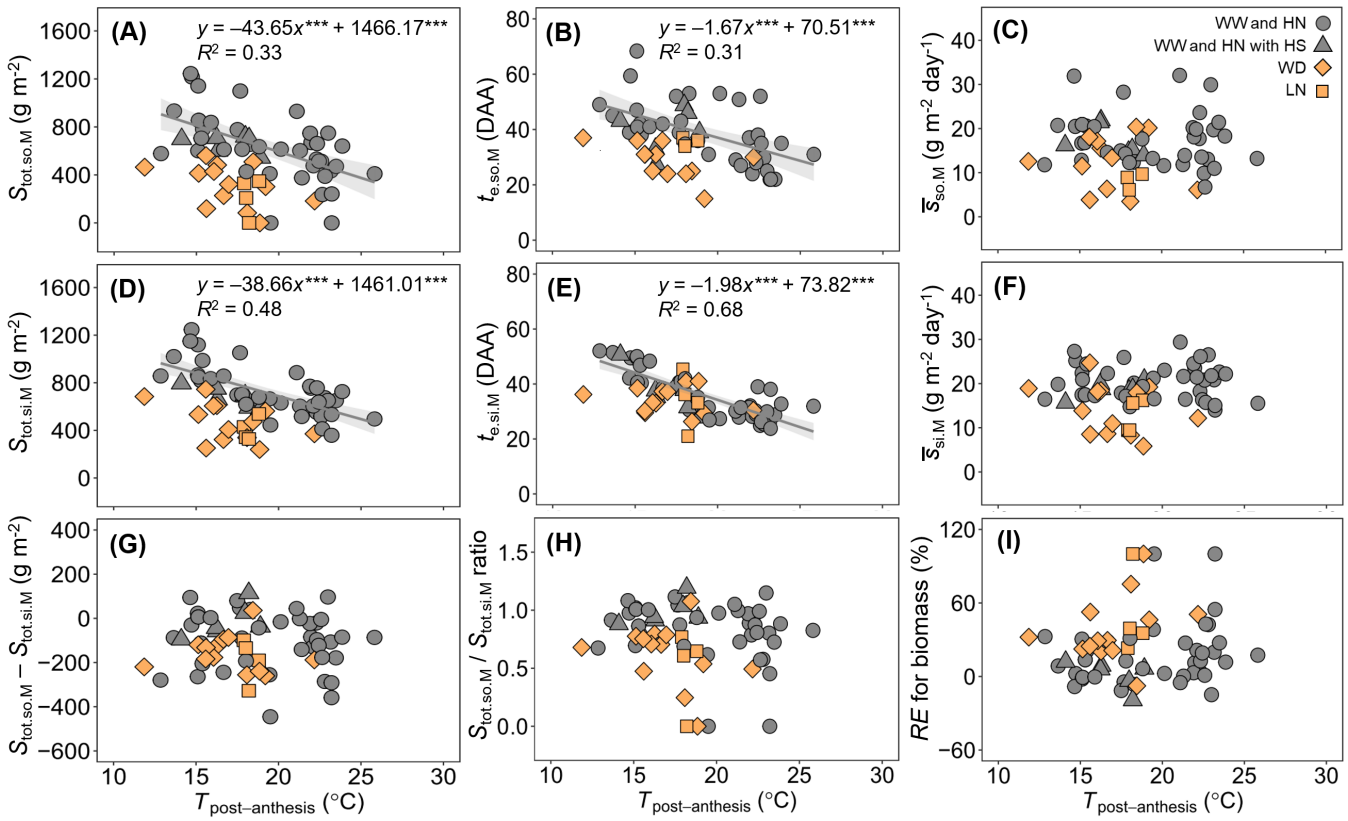

Fig. 5. Post-anthesis source and sink parameters for biomass (M) versus average daily temperature of the period. (A–C) Temperature responses of total source supply ($S_{tot.so.M}$), days after anthesis when the source activity has decreased to zero ($t_{e.so.M}$), and mean source activity ($\bar{s}_{so.M}$) for biomass. (D–F) Temperature responses of total sink demand ($S_{tot.si.M}$), days after anthesis when the daily sink strength has decreased to zero ($t_{e.si.M}$), and mean sink strength ($\bar{s}_{si.M}$) for biomass. (G–I) Temperature responses of the difference between $S_{tot.so.M}$ and $S_{tot.si.M}$, the ratio of $S_{tot.so.M}$ to $S_{tot.si.M}$, and the contribution of remobilized pre-anthesis assimilates to final grain dry mass (RE for biomass). Lines are linear regression fitted to the data for the well-watered and high nitrogen supply regimes and are shown only when significant at P=0.05. *** indicates statistical significance at P<0.001. The shaded area depicts the 95% confidence interval of the predictions for the conditions well-watered and high nitrogen supply regimes. WW, well-watered; WD, water deficit; HN, non-limiting nitrogen; LN, low nitrogen supply; HS, heat shock.

that total post-anthesis nitrogen uptake ($S_{tot.so.N}$), total grain nitrogen accumulation ($S_{tot.si.N}$), and their difference or ratio were insensitive to $T_{post-anthesis}$ and water supply (Fig. 6A, D, G, H), and RE for nitrogen was roughly constant across $T_{post-anthesis}$ and water regimes (Fig. 6I). This was also in agreement with previous findings that nitrogen partitioning is unaffected by post-anthesis heat and drought in wheat (Triboï *et al.*, 2003), and that nitrogen relationships during grain filling are little affected by shading applied after stem elongation in wheat (Shao *et al.*, 2021). In fact, most regimes in our study were imposed after anthesis (Fig. 1), when crops had already taken up sufficient nitrogen for filling grains, implying that environmental changes during the post-anthesis period would have limited impacts on the amount of available nitrogen for remobilization, and thus on total grain nitrogen accumulation ($S_{tot.si.N}$). As a result, we also observed an increased $\bar{s}_{si.N}$, mainly due to an increased remobilization of nitrogen, that could have compensated for the decreased grain nitrogen accumulation duration ($t_{e.si.N}$) with increasing $T_{post-anthesis}$ (Fig. 6E, F). A similar compensation between the rate and duration of grain nitrogen accumulation for wheat in response to post-anthesis temperature was observed by Dupont *et al.* (2006).

While we observed that total grain nitrogen accumulation ($S_{tot.si.N}$) positively correlated with total grain biomass ($S_{tot.si.M}$) (Supplementary Fig. S8B), this did not necessarily imply that they respond similarly to environmental variables (Panozzo and Eagles, 1999; Dupont *et al.*, 2006). High temperatures and WD reduced $S_{tot.si.M}$ and average final grain dry mass (Fig. 5D; Supplementary Fig. S9A), but did not significantly affect $S_{tot.si.N}$ (Fig. 6D) and average final nitrogen mass per grain (Supplementary Fig. S9E), leading to an increase in grain nitrogen concentration (Supplementary Fig. S9D). Many previous studies (e.g. Kimball *et al.*, 2001; Yin *et al.*, 2009) also showed this. Given that high temperatures and WD mostly occur during the post-anthesis period in most wheat-growing regions (Asseng *et al.*, 2019), our results implied that a future warmer and drier climate may not lower grain nitrogen/protein concentration of wheat. This was in agreement with the advocacy of recent studies that the combined elevated temperature and elevated CO_2 would not result in lower grain

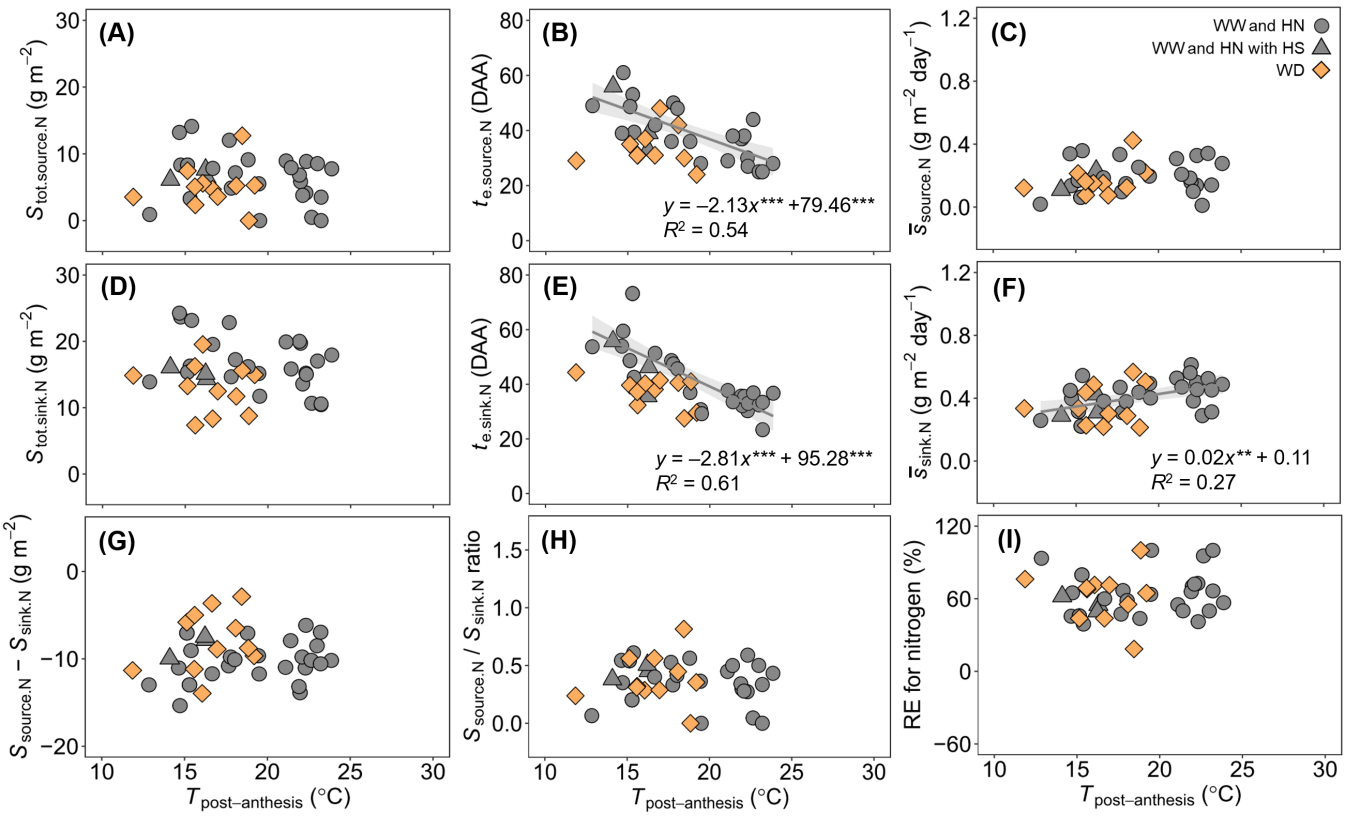

Fig. 6. Post-anthesis source and sink parameters for nitrogen (N) versus average daily temperature of the period. (A–C) Temperature responses of total source supply ($S_{tot.so.N}$), days after anthesis when the source activity has decreased to zero ($t_{e.so.N}$), and mean source activity ($\bar{s}_{so.N}$) for nitrogen. (D–F) Temperature responses of total sink demand ($S_{tot.si.N}$), days after anthesis when the daily sink strength has decreased to zero ($t_{e.si.N}$), and mean sink strength ($\bar{s}_{si.N}$) for nitrogen. (G–I) Temperature responses of the difference between $S_{tot.so.N}$ and $S_{tot.si.N}$, the ratio of $S_{tot.so.N}$ to $S_{tot.si.N}$, and the contribution of remobilized pre-anthesis nitrogen to final grain nitrogen mass (RE for nitrogen). Lines are linear regression fitted to the data for the well-watered and high nitrogen supply regimes and are shown only when significant at P=0.05. ** and *** indicate statistical significance at P<0.01 and 0.001, respectively. The shaded area depicts the 95% confidence interval of the predictions. WW, well-watered; WD, water deficit; HN, non-limiting nitrogen; HS, heat shock.

nutritional quality for wheat and rice (Wang *et al.*, 2019, 2020; Guo *et al.*, 2022), but was in contrast to earlier reports (e.g. Myers *et al.*, 2014 who only considered the elevated CO_2 effect) that climate change threatens grain quality.

Post-anthesis source–sink relationships were genotype dependent

The responses of crops to environmental variables are often genotype dependent (Chenu *et al.*, 2017; Eller *et al.*, 2020; Jiang *et al.*, 2022; Wang *et al.*, 2022). Here, by assessing the responses to HT, WD, and LN regimes of four winter wheat genotypes with contrasting sink–source ratios (Supplementary Figs S5, S6), we showed that these contrasting genotypes had different strategies (by adjusting their source–sink relationships) to cope with these adverse conditions. For instance, under adverse conditions, Arche maintained its post-anthesis assimilation rate ($\bar{s}_{so.M}$; Supplementary Fig. S5D), while Récital and Renan had higher RE for biomass than under favorable conditions (Supplementary Fig. S5A, B, D). In addition, although HT generally did not significantly alter biomass relationships for all genotypes, it impacted post-anthesis above-ground biomass accumulation ($S_{tot.so.M}$) and grain biomass accumulation ($S_{tot.si.M}$) differently among genotypes. For instance, HT impacts were large for Arche but minimal for Renan (Supplementary Fig. S5A).

Since Tamaro hardly accumulated above-ground biomass over the whole grain-filling period (i.e. $S_{tot.so.M}$ was assumed to be zero), an extremely high remobilization of pre-anthesis assimilates (RE for biomass was close to 100%) was always demanded regardless of growth conditions (Fig. 4A; Supplementary Fig. S5A). For nitrogen, on the other hand, while pre-anthesis nitrogen remobilization was always needed among environments and genotypes, the sensitivities of post-anthesis above-ground nitrogen accumulation ($S_{tot.so.N}$) and grain nitrogen accumulation ($S_{tot.si.N}$) to temperature and water availability varied among genotypes (Supplementary Fig. S6). Hence, taken together, to obtain reliable insights for assisting breeding, genotypic differences in these traits should simultaneously be assessed, particularly for biomass.

Concluding remarks

By systematically assessing wheat post-anthesis source–sink relationships, our study showed that the remobilization of pre-anthesis reserves became increasingly important for grain growth with increasing stress intensity. Our study also revealed that overall, WD and LN exerted a greater impact on wheat source–sink relationships than high temperature, suggesting the greater importance of water availability relative to rising temperatures for grain growth under our experimental conditions. Thus, improving photosynthesis (source) as well as the remobilization of reserve assimilates under drought and the combination of drought and heat appeared to be important for increasing productivity under climate change. Also, our study suggested that warmer and drier future climates may not threaten the quality of wheat grain in terms of protein concentration (Supplementary Fig. S9D). Finally, to reduce the uncertainty in assessing future climate change impacts, efforts to understand the interactions of multiple (non-)environmental factors (e.g. temperature×water×CO_2×fertilization×genotype), rather than the impact of a single or merely two factors, are needed (Mittler, 2006; Suzuki *et al.*, 2014; Webber *et al.*, 2022).

Supplementary data

The following supplementary data are available at *JXB* online.

Table S1. Metainformation of the experiments used in this study.

Protocol S1. SAS scripts for simultaneous estimation of post-anthesis source and sink parameters.

Fig. S1. Estimated source–sink parameters for biomass as affected by 'Temperature' factor.

Fig. S2. Estimated source–sink parameters for nitrogen as affected by 'Temperature' factor.

Fig. S3. Estimated source–sink parameters for biomass as affected by 'Water' factor.

Fig. S4. Estimated source–sink parameters for nitrogen as affected by 'Water' factor.

Fig. S5. Estimated source–sink parameters for biomass of different genotypes.

Fig. S6. Estimated source–sink parameters for nitrogen for different genotypes.

Fig. S7. Relationships between post-anthesis source and sink components for wheat genotypes grown under different regimes.

Fig. S8. Relationships of post-anthesis source supply and sink demand for biomass and nitrogen.

Fig. S9. Temperature responses of yield and production traits for either biomass or nitrogen.

Author contributions

XY and PM: conceived the study; CG and PM: conceived the experimentation; LF and PM: sorted out raw data archives; XY: designed the model methods; LF: conducted analyses and wrote the draft; PCS, CG, XY, and PM: revised the manuscript.

Conflict of interest

The authors have no conflicts to declare.

Funding

None.

Data availability

The data that support the findings of this study are openly available at the Dryad Digital Repository (https://doi.org/10.5061/dryad.9ghx3ffrw) (Fang *et al.*, 2024)

References

Asseng S, Ewert F, Martre P, *et al*. 2015. Rising temperatures reduce global wheat production. Nature Climate Change **5**, 143–147.

Asseng S, Kassie BT, Labra MH, Amador C, Calderini DF. 2017. Simulating the impact of source–sink manipulations in wheat. Field Crops Research **202**, 47–56.

Asseng S, Martre P, Maiorano A, *et al*. 2019. Climate change impact and adaptation for wheat protein. Global Change Biology **25**, 155–173.

Barbottin A, Lecomte C, Bouchard C, Jeuffroy MH. 2005. Nitrogen remobilization during grain filling in wheat: genotypic and environmental effects. Crop Science **45**, 1141–1150.

Barnabás B, Jäger K, Fehér A. 2008. The effect of drought and heat stress on reproductive processes in cereals. Plant, Cell & Environment **31**, 11–38.

Chenu K, Porter JR, Martre P, Basso B, Chapman SC, Ewert F, Bindi M, Asseng S. 2017. Contribution of crop models to adaptation in wheat. Trends in Plant Science **22**, 472–490.

de Oliveira ED, Bramley H, Siddique KH, Henty S, Berger J, Palta JA. 2012. Can elevated CO_2 combined with high temperature ameliorate the effect of terminal drought in wheat? Functional Plant Biology **40**, 160–171.

Dingkuhn M, Luquet D, Fabre D, Muller B, Yin X, Paul M. 2020. The case for improving crop carbon sink strength or plasticity for a CO_2-rich future. Current Opinion in Plant Biology **56**, 259–272.

Dupont FM, Hurkman WJ, Vensel WH, Tanaka C, Kothari KM, Chung OK, Altenbach SB. 2006. Protein accumulation and composition in wheat grains: effects of mineral nutrients and high temperature. European Journal of Agronomy **25**, 96–107.

Eller F, Hyldgaard B, Driever SM, Ottosen CO. 2020. Inherent trait differences explain wheat cultivar responses to climate factor interactions: new insights for more robust crop modelling. Global Change Biology **26**, 5965–5978.

Evans LT. 1993. Crop evolution, adaptation and yield. Cambridge, UK: Cambridge University Press.

Fang L, Martre P, Jin K, Du X, van der Putten PE, Yin X, Struik PC. 2023. Neglecting acclimation of photosynthesis under drought can cause significant errors in predicting leaf photosynthesis in wheat. Global Change Biology **29**, 505–521.

Fang L, Struik PC, Girousse C, Yin X, Martre P. 2024. Data from: Source–sink relationships during grain filling in wheat in response to various temperature, water deficit, and nitrogen deficit regimes [Dataset]. Dryad. https://doi.org/10.5061/dryad.9ghx3ffrw

FAOSTAT. 2022. Statistics 2022. https://www.fao.org/faostat/en/#home

Farooq M, Hussain M, Siddique KH. 2014. Drought stress in wheat during flowering and grain-filling periods. Critical Reviews in Plant Sciences **33**, 331–349.

Gebbing T, Schnyder H. 1999. Pre-anthesis reserve utilization for protein and carbohydrate synthesis in grains of wheat. Plant Physiology **121**, 871–878.

Guo X, Huang B, Zhang H, *et al*. 2022. T-FACE studies reveal that increased temperature exerts an effect opposite to that of elevated CO_2 on nutrient concentration and bioavailability in rice and wheat grains. Food and Energy Security **11**, e336.

Jiang D, Mulero G, Bonfil DJ, Helman D. 2022. Early or late? The role of genotype phenology in determining wheat response to drought under future high atmospheric CO_2 levels. Plant, Cell & Environment **45**, 3445–3461.

Kichey T, Hirel B, Heumez E, Dubois F, Le Gouis J. 2007. In winter wheat (*Triticum aestivum* L.), post-anthesis nitrogen uptake and remobilisation to the grain correlates with agronomic traits and nitrogen physiological markers. Field Crops Research **102**, 22–32.

Kimball BA, Morris CF, Pinter Jr PJ, *et al*. 2001. Elevated CO_2, drought and soil nitrogen effects on wheat grain quality. New Phytologist **150**, 295–303.

Lesk C, Anderson W, Rigden A, Coast O, Jägermeyr J, McDermid S, Davis KF, Konar M. 2022. Compound heat and moisture extreme impacts on global crop yields under climate change. Nature Reviews. Earth & Environment **3**, 872–889.

Liu B, Liu L, Tian L, Cao W, Zhu Y, Asseng S. 2014. Post-heading heat stress and yield impact in winter wheat of China. Global Change Biology **20**, 372–381.

Liu J, Hu T, Fang L, Peng X, Liu F. 2019. CO_2 elevation modulates the response of leaf gas exchange to progressive soil drying in tomato plants. Agricultural and Forest Meteorology **268**, 181–188.

Martre P, Porter JR, Jamieson PD, Triboi E. 2003. Modeling grain nitrogen accumulation and protein composition to understand the sink/source regulations of nitrogen remobilization for wheat. Plant Physiology **133**, 1959–1967.

Mittler R. 2006. Abiotic stress, the field environment and stress combination. Trends in Plant Science **11**, 15–19.

Myers SS, Zanobetti A, Kloog I, *et al*. 2014. Increasing CO_2 threatens human nutrition. Nature **510**, 139–142.

Nicolas ME, Gleadow RM, Dalling MJ. 1984. Effects of drought and high temperature on grain growth in wheat. Functional Plant Biology **11**, 553–566.

Palta JA, Kobata T, Turner NC, Fillery IR. 1994. Remobilization of carbon and nitrogen in wheat as influenced by postanthesis water deficits. Crop Science **34**, 118–124.

Panozzo JF, Eagles HA. 1999. Rate and duration of grain filling and grain nitrogen accumulation of wheat cultivars grown in different environments. Australian Journal of Agricultural Research **50**, 1007–1015.

Papakosta DK, Gagianas AA. 1991. Nitrogen and dry matter accumulation, remobilization, and losses for Mediterranean wheat during grain filling. Agronomy Journal **83**, 864–870.

Penning de Vries FWT, Jansen DM, ten Berge HFM, Bakema A. 1989. Simulation of ecophysiological processes of growth in several annual crops. Los Banos: IRRI and Wageningen: Pudoc.

Pinto RS, Reynolds MP, Mathews KL, McIntyre CL, Olivares-Villegas JJ, Chapman SC. 2010. Heat and drought adaptive QTL in a wheat population designed to minimize confounding agronomic effects. Theoretical and Applied Genetics **121**, 1001–1021.

Reynolds MP, Slafer GA, Foulkes JM, Griffiths S, Murchie EH, Carmo-Silva E, Flavell RB. 2022. A wiring diagram to integrate physiological traits of wheat yield potential. Nature Food **3**, 318–324.

Rogers GS, Milham PJ, Gillings M, Conroy JP. 1996. Sink strength may be the key to growth and nitrogen responses in N-deficient wheat at elevated CO_2. Functional Plant Biology **23**, 253–264.

Schapendonk AHCM, Xu HY, Van Der Putten PEL, Spiertz JHJ. 2007. Heat-shock effects on photosynthesis and sink–source dynamics in wheat (*Triticum aestivum* L.). NJAS: Wageningen Journal of Life Sciences **55**, 37–54.

Shao L, Liu Z, Li H, *et al*. 2021. The impact of global dimming on crop yields is determined by the source–sink imbalance of carbon during grain filling. Global Change Biology **27**, 689–708.

Shi W, Xiao G, Struik PC, Jagadish KS, Yin X. 2017. Quantifying source–sink relationships of rice under high night-time temperature combined with two nitrogen levels. Field Crops Research **202**, 36–46.

Shiferaw B, Smale M, Braun HJ, Duveiller E, Reynolds M, Muricho G. 2013. Crops that feed the world 10. Past successes and future challenges to the role played by wheat in global food security. Food Security **5**, 291–317.

Sinclair TR, de Wit CT. 1975. Photosynthate and nitrogen requirements for seed production by various crops. Science **189**, 565–567.

Stone PJ, Nicolas ME. 1995. Effect of timing of heat stress during grain filling on two wheat varieties differing in heat tolerance. I. Grain growth. Functional Plant Biology **22**, 927–934.

Suzuki N, Rivero RM, Shulaev V, Blumwald E, Mittler R. 2014. Abiotic and biotic stress combinations. New Phytologist **203**, 32–43.

Tilman D, Balzer C, Hill J, Befort BL. 2011. Global food demand and the sustainable intensification of agriculture. Proceedings of the National Academy of Sciences, USA **108**, 20260–20264.

Triboï E, Martre P, Triboï-Blondel AM. 2003. Environmentally-induced changes in protein composition in developing grains of wheat are related to changes in total protein content. Journal of Experimental Botany **54**, 1731–1742.

Triboï E, Triboï-Blondel A, Martignac M, Falcimagne R. 1996. Experimental device for studying post-anthesis canopy functioning in relation to grain quality. In: Proceedings of the 4th European Society of Agronomy Congress, Wageningen, The Netherlands, 68–69.

Wang J, Hasegawa T, Li L, Lam SK, Zhang X, Liu X, Pan G. 2019. Changes in grain protein and amino acids composition of wheat and rice under short-term increased [CO_2] and temperature of canopy air in a paddy from East China. New Phytologist **222**, 726–734.

Wang J, Li L, Lam SK, Liu X, Pan G. 2020. Responses of wheat and rice grain mineral quality to elevated carbon dioxide and canopy warming. Field Crops Research **249**, 107753.

Wang X, Li X, Zhong Y, Blennow A, Liang K, Liu F. 2022. Effects of elevated CO_2 on grain yield and quality in five wheat cultivars. Journal of Agronomy and Crop Science **208**, 733–745.

Wardlaw IF, Moncur LJFPB. 1995. The response of wheat to high temperature following anthesis. I. The rate and duration of kernel filling. Functional Plant Biology **22**, 391–397.

Webber H, Martre P, Asseng S, *et al*. 2017. Canopy temperature for simulation of heat stress in irrigated wheat in a semi-arid environment: a multi-model comparison. Field Crops Research **202**, 21–35.

Webber H, Rezaei EE, Ryo M, Ewert F. 2022. Framework to guide modeling single and multiple abiotic stresses in arable crops. Agriculture, Ecosystems & Environment **340**, 108179.

Wei H, Meng T, Li X, Dai Q, Zhang H, Yin X. 2018. Sink–source relationship during rice grain filling is associated with grain nitrogen concentration. Field Crops Research **215**, 23–38.

Wei Z, Abdelhakim LOA, Fang L, Peng X, Liu J, Liu F. 2022. Elevated CO_2 effect on the response of stomatal control and water use efficiency in amaranth and maize plants to progressive drought stress. Agricultural Water Management **266**, 107609.

Wei Z, Fang L, Li X, Liu J, Liu F. 2020. Effects of elevated atmospheric CO_2 on leaf gas exchange response to progressive drought in barley and tomato plants with different endogenous ABA levels. Plant and Soil **447**, 431–446.

Winkel T, Renno JF, Payne WA. 1997. Effect of the timing of water deficit on growth, phenology and yield of pearl millet (*Pennisetum glaucum* (L.) R. Br.) grown in Sahelian conditions. Journal of Experimental Botany **48**, 1001–1009.

Yang J, Zhang J. 2006. Grain filling of cereals under soil drying. New Phytologist **169**, 223–236.

Yang J, Zhang J, Liu K, Wang Z, Liu L. 2006. Abscisic acid and ethylene interact in wheat grains in response to soil drying during grain filling. New Phytologist **171**, 293–303.

Yang W, Peng S, Dionisio-Sese ML, Laza RC, Visperas RM. 2008. Grain filling duration, a crucial determinant of genotypic variation of grain yield in field-grown tropical irrigated rice. Field Crops Research **105**, 221–227.

Yin X, Goudriaan J, Lantinga EA, Vos J, Spiertz JHJ. 2003. A flexible sigmoid function of determinate growth. Annals of Botany **91**, 361–371.

Yin X, Guo W, Spiertz JHJ. 2009. A quantitative approach to characterize sink–source relationships during grain filling in contrasting wheat genotypes. Field Crops Research **114**, 119–126.

Yin X, Struik PC. 2017. Can increased leaf photosynthesis be converted into higher crop mass production? A simulation study for rice using the crop model GECROS. Journal of Experimental Botany **68**, 2345–2360.

Yin X, Struik PC, Goudriaan J. 2021. On the needs for combining physiological principles and mathematics to improve crop models. Field Crops Research **271**, 108254.

Zhang S, Wang H, Fan J, Zhang F, Cheng M, Yang L, Ji Q, Li Z. 2022. Quantifying source–sink relationships of drip-fertigated potato under various water and potassium supplies. Field Crops Research **285**, 108604.

Zhao C, Liu B, Piao S, *et al*. 2017. Temperature increase reduces global yields of major crops in four independent estimates. Proceedings of the National Academy of Sciences, USA **114**, 9326–9331.

Zhao H, Dai T, Jing Q, Jiang D, Cao W. 2007. Leaf senescence and grain filling affected by post-anthesis high temperatures in two different wheat cultivars. Plant Growth Regulation **51**, 149–158.